Molecular Pharmacology Fast Forward. Published on March 28, 2014 as doi:10.1124/mol.114.091603
This article has not been copyedited and formatted. The final version may differ from this version.

Epirubicin upregulates UDP Glucuronosyltransferase 2B7 expression in liver cancer cells via the p53 pathway

Dong Gui Hu, Anne Rogers, and Peter I Mackenzie

Department of Clinical Pharmacology, Flinders University School of Medicine, Flinders Medical Centre, Bedford Park SA 5042, Australia (DGH, AR, PIM)

Molecular Pharmacology Fast Forward. Published on March 28, 2014 as DOI: 10.1124/mol.114.091603
This article has not been copyedited and formatted. The final version may differ from this version.

Running Title: Upregulation of *UGT2B7* by epirubicin in liver cancer cells

Address correspondence to author: Peter I Mackenzie

Dr. Peter I. Mackenzie, Department of Clinical Pharmacology, Flinders Medical Centre, Bedford Park, SA 5042, Australia.

Phone: 0061 8 8204 5394

Fax: 0061 8 8204 5114

E-mail: peter.mackenzie@flinders.edu.au

Number of text pages: 37

Number of Tables: 1

Number of figures: 8

Number of references: 49

Word count (Abstract): 245

Word count (Introduction): 708

Word count (discussion): 1504

The abbreviations used are: Caco-2, human colorectal adenocarcinoma cell line; CHF, congestive heart failure; ChIP-qPCR, chromatin immunoprecipitation assay and quantitative real-time PCR; CYP, cytochrome p450; DOX, doxorubicin; DNR, daunorubicin; EPI, epirubicin; FXR, farnesoid X receptor; HCC, hepatocellular carcinoma; IDA, idarubicin; OATP1B1, organic anion-transporting polypeptide 1B1; p53, tumour suppressor p53 protein; p53RE, p53 response element; RT-qPCR, reverse transcriptase quantitative real-time PCR; siRNA, small interfering RNA; UGT, UDP-glucuronosyltransferase; UDPGA, UDP-glucuronic acid.

Molecular Pharmacology Fast Forward. Published on March 28, 2014 as DOI: 10.1124/mol.114.091603
This article has not been copyedited and formatted. The final version may differ from this version.

Abstract

Anthracyclines are effective genotoxic anticancer drugs for treating human malignancies; however, their clinical use is limited by tumour resistance and severe cardiotoxicity (e.g. congestive heart failure). Epirubicin (EPI) is less cardiotoxic compared to other canonical anthracyclines (e.g, doxorubicin). This has been attributed to its unique glucuronidation detoxification pathway. EPI is primarily inactivated by UDP-glucuronosyltransferase 2B7 (UGT2B7) in the liver. Hence, the regulation of hepatic *UGT2B7* expression is critical for EPI systemic clearance but remains poorly characterized. We show herein that EPI upregulates *UGT2B7* expression in hepatocellular carcinoma (HCC) HepG2 and Huh7 cells. Our analyses of deleted and mutated *UGT2B7* promoter constructs identified a p53 response element (p53RE) in the *UGT2B7* promoter. EPI stimulated *UGT2B7* promoter activity via this p53RE and enhanced in vivo p53 binding at this p53RE in HepG2 cells. Knockdown of p53 expression by siRNA silencing technology significantly repressed the capacity of EPI to stimulate *UGT2B7* transcription. Furthermore, the p53 activator nutlin-3α significantly enhanced *UGT2B7* expression and recruited the p53 protein to the *UGT2B7* p53RE in HepG2 cells. Collectively, our results demonstrated that EPI promotes its own detoxification via the p53-mediated pathway. This regulation may contribute to tumour resistance to EPI-containing HCC chemotherapy and may also provide a new explanation for the reduced cardiotoxicity of EPI compared to other anthracyclines. Our finding also suggests that upon exposure to genotoxic agents, detoxifying genes are activated by the p53-mediated pathway to clear genotoxic agents locally within the tumour site or even systemically through the liver.

Molecular Pharmacology Fast Forward. Published on March 28, 2014 as DOI: 10.1124/mol.114.091603
This article has not been copyedited and formatted. The final version may differ from this version.

Introduction

Anthracyclines are among the most effective anticancer drugs. Doxorubicin (DOX), daunorubicin (DNR), epirubicin (EPI), and idarubicin (IDA) are classic anthracyclines, which share a typical quinone-containing tetracyclic aromatic ring structure with a sugar moiety, namely daunosamine, attached at the C-7 of ring A through a glycosidic bond (Ormrod et al. 1999). DNR was the first anthracycline that was initially isolated from *Streptomyces peuceticus* cultures. Structural modification of the DNR led to DOX (hydroxylation at C-14) and IDA (demethoxylation at C-4). EPI is an epimer of DOX with the C'-4 hydroxyl group on the sugar being axial in DOX and equatorial in EPI (Ormrod et al. 1999). DNR and IDA are generally restricted to treatment of acute myeloid leukemias and acute myelogenous leukemia, respectively (Piekarski and Jelinska 2013). In contrast, DOX and EPI have a broader spectrum of anticancer activities with similar equimolar efficacy for treating various solid tumours and haematological malignancies (Minotti et al. 2004).

Chronic administration of anthracyclines induces irreversible cardiomyopathy that leads to congestive heart failure (CHF), and this limits their clinical use (Minotti et al. 2004). To avoid CHF, a maximum cumulative dose of ~500 mg/m^2 for anthracyclines (e.g. DOX) has been recommended for clinical use (Minotti et al. 2004). In contrast, EPI has a higher recommended maximum cumulative dose of ~900 mg/m^2. This allows more treatment cycles of EPI with no extra toxicity (Minotti et al. 2004). Anthracyclines are intensively metabolized in the liver. Classic anthracyclines can be converted to the less cytotoxic carbon-13 dihydroderivatives (e.g. doxorubicinol, epirubicinol, daunorubicinol, and idarubicinol) by aldoketoreductases (Jin and Penning 2007) or carbonyl reductases (Bains et al. 2009). This represents the major metabolic pathway for DOX, DNR, and IDA (Le Bot et al. 1988). In contrast, with an equatorially positioned C'-4 hydroxyl group that permits glucuronidation,

Molecular Pharmacology Fast Forward. Published on March 28, 2014 as DOI: 10.1124/mol.114.091603
This article has not been copyedited and formatted. The final version may differ from this version.

EPI can be converted to EPI-glucuronide. After administration, EPI-glucuronide is the major metabolite of EPI in plasma and bile (Minotti et al. 2004). EPI-glucuronide is not cardiotoxic and is rapidly excreted from the body (Ormrod et al. 1999). The reduced cardiotoxicity of EPI has been attributed to its unique glucuronidation clearance pathway (Ormrod et al. 1999).

Glucuronidation, which is carried out by UDP-glucuronosyltransferases (UGTs), has an important role in drug detoxification and clearance. Human UGTs are classified into subfamilies based on their amino acid sequence homology (Mackenzie et al. 2005, Mackenzie et al. 1997). Glucuronidation of EPI is primarily carried out by UGT2B7 in the liver (Innocenti et al. 2001, Ormrod et al. 1999). As a result, factors that modulate hepatic *UGT2B7* expression and activity would have potential impact on EPI systemic clearance. EPI is used to treat hepatocellular carcinoma (HCC) and a variety of non-hepatic human malignancies. In terms of intratumoral detoxification of EPI, upregulation of *UGT2B7* in cancer cells by EPI would be clinical relevant. Furthermore, a possible upregulation of *UGT2B7* by EPI in a cancerous or even normal hepatic cellular context would be more significant as this would promote EPI systemic clearance when EPI is administered to patients with non-hepatic cancers (e.g. breast cancer). These hypotheses remain to be investigated.

The tumour suppressor p53 protein is well-known for its role in suppressing carcinogenesis. This is partly because of its ability to activate a variety of genes that are involved in DNA repair and apoptosis in response to DNA damage. p53 is a transcription factor and regulates its target gene transcription by binding to p53 response elements (p53RE) that are present in target gene promoters and enhancers. A canonical p53RE contains two 10-base decamers RRRCWWGYYY that are separated by a spacer of 0-21 (R is a purine; Y is a pyrimidine; W is A or T) (Riley et al. 2008). Upon activation, p53 binds as a tetramer with each p53 protein

Molecular Pharmacology Fast Forward. Published on March 28, 2014 as DOI: 10.1124/mol.114.091603
This article has not been copyedited and formatted. The final version may differ from this version.

interacting with one pentamer of RRRCW or WGYYY at the site to activate or repress target gene transcription (Menendez, Inga and Resnick 2009, Riley et al. 2008).

In the present study, we reported that EPI stimulates the expression and activity of the UGT2B7 enzyme in HCC cell lines. We further demonstrated that in the HepG2 cell line, the most frequently used hepatic model cell line, EPI promotes *UGT2B7* gene transcription via p53 binding to a p53RE in its proximal promoter. This study identifies *UGT2B7* as a novel p53 target gene.

Molecular Pharmacology Fast Forward. Published on March 28, 2014 as DOI: 10.1124/mol.114.091603
This article has not been copyedited and formatted. The final version may differ from this version.

Materials and Methods

Materials. Epirubicin, nutlin-3α, cycloheximide, actinomycin D, morphine, UDP-glucuronic acid (UDPGA), were all purchased from Sigma-Aldrich (St. Louis, MO). Primers were synthesized by Sigma-Genosys (Castle Hill, NSW, Australia). Restriction endonucleases (KpnI, MulI, and XhoI) were purchased from New England Biolabs.

Cell Treatment, RNA extraction, and Reverse Transcriptase Quantitative Real-Time PCR (RT-qPCR). The hepatocellular carcinoma HepG2 cell line was purchased from ATCC and the Huh-7 cell line was obtained from Dr Jillian Carr (Flinders University, Adelaide, Australia). Both cell lines were maintained in DMEM containing 10% FBS at 37 °C in a 5% CO_2 atmosphere. For drug treatment, cells were plated in six-well plates and cultured for 3-4 days when they reached approximately 80% confluence. Cells were then treated with drugs in triplicate at concentrations and lengths of time as indicated in the Figures. Total RNA was extracted using the RNeasy Mini Kit (QIAGEN, Valencia, CA) and the resultant RNA was used to generate cDNA using Invitrogen reverse transcription reagents as previously reported (Hu and Mackenzie 2009). Real-time PCR was performed using a RotorGene 3000 instrument (Corbett Research, NSW, Australia) in a 20 µl-reaction of 1xQuantiTect SYBR Green PCR master mix (QIAgen) containing ~60 ng of cDNA sample and a pair of gene-specific primers (500 nM for each primer). The primers and the methods used to quantify the transcript levels of UGTs, β-actin, and 18S rRNA were previously described (Congiu et al. 2002, Hu et al. 2010, Hu and Mackenzie 2009, Hu and Mackenzie 2010). The mRNA levels of *p21* and *CYP3A4* relative to 18S rRNA were quantified using the $2^{-\Delta\Delta Ct}$ method (Livak and Schmittgen 2001). The PCR primers for *p21* and *CYP3A4* are given in Table 1.

Molecular Pharmacology Fast Forward. Published on March 28, 2014 as DOI: 10.1124/mol.114.091603
This article has not been copyedited and formatted. The final version may differ from this version.

Generation of UGT2B7 Promoter Luciferase Reporter Deletion Constructs and Mutants. Eleven pGL3-derived luciferase reporter constructs carrying varying lengths of the *UGT2B7* promoter were used in transient transfection in this study (Fig. 4). Four of these constructs were previously reported, namely 2B7-44/+59, 2B7-132/+59, 2B7-275/+59, and 2B7-516/+59 (Gregory et al. 2006, Ishii, Hansen and Mackenzie 2000). Nucleotides of promoter constructs were numbered from the transcription start site in these studies. These constructs were renamed herein as 2B7-103/-1, 2B7-191/-1, 2B7-334/-1, and 2B7-575/-1 by numbering nucleotide +1 as the A of the initiation codon, as recommended by the Gene Nomenclature Committee. In the present study, two promoter fragments, -240/-1 and -283/-1 were amplified from the 2B7-575/-1 construct with Phusion hot start high-fidelity DNA polymerase (Thermo Fisher Scientific, Pittsburgh, PA) and cloned into the KpnI site of the pGL3-basic vector generating two constructs (2B7-240/-1 and 2B7-283/-1) (Fig. 4B). Five *UGT2B7* promoter fragments (-1046/-1, -2076/-1, -3026/-1, -4026/-1, and -4926/-1) were further amplified from a commercial genomic DNA sample (Roche) and cloned into the MulI and XhoI sites of the pGL3-basic vector generating five reporter constructs (2B7-1046/-1, 2B7-2076/-1, 2B7-3026/-1, 2B7-4026/-1, and 2B7-4926/-1, respectively). Sequencing of the cloned promoter fragments showed that their sequences all matched the *UGT2B7* promoter reference sequence (NC-000004.11). As depicted in Fig. 4C, the 51-bp promoter region between nucleotides -288 and -238 in the 2B7-575/-1 reporter construct was mutated at five positions using the QuickChange site-directed mutagenesis kit (Stratagene, La Jolla, CA) to generate five mutants (-575/-TM1-5). The sequences of primers for PCR, sequencing, cloning, and mutagenesis are given in Table 1.

Transient Transfection and Luciferase Reporter Assay. Exponentially growing HepG2 cells were trypsinized and subsequently plated into 96-well plates in 100 µl of DMEM

Molecular Pharmacology Fast Forward. Published on March 28, 2014 as DOI: 10.1124/mol.114.091603
This article has not been copyedited and formatted. The final version may differ from this version.

supplemented with 10% FBS. 50 µl of transfection mixture containing 200 ng of each reporter construct, 8 ng of pRL-null vector (Premega), and 0.8 µl of Lipofectamine 2000 (Invitrogen) were added to each well when the culture reached approximately 60% confluence. 24 h after transfection, the transfection medium was removed and cells were treated with 1 µM EPI or vehicle (0.1% ethanol) for 24 h. Cells were then lysed for luciferase assays using the Dual-Luciferase Reporter Assay System (Promega, Madison, WT) according to the manufacturer's instructions as previously described (Hu and Mackenzie 2009).

Small Interfering RNA Knockdown Experiments. On-TARGETplusSMARTpool small interfering RNA (siRNA) against p53 and On-TARGETplus nontargeting pool siRNA (nontarget siRNA) were purchased from Dharmacon RNAi Technologies (Lafayette, CO). For transfection assays, 1.5 ml of fresh DMEM containing HepG2 cells ($3x10^5$) was combined with 0.5 ml of serum-free DMEM medium containing 10 µl of Lipofectamine 2000 and 10 ul of anti-p53 siRNA (20 µM) or nontarget siRNA (20 µM) and subsequently plated into six-well plates. Each transfection was conducted in four wells. 24 h after transfection, the medium was removed and cells were incubated for another 24 h in fresh DMEM medium. 48 h post-transfection, cells were harvested from one well of each transfection for western blotting assays as described below. The remaining three wells of each transfection were treated with 1 µM EPI or vehicle (0.1% ethanol) for 24 h. Cells were then harvested for total RNA, followed by RT-qPCR to quantify target mRNA levels as described above.

Western Blotting. Whole cell lysates were prepared from EPI (or vehicle)-treated HepG2 cells or anti-p53 siRNA (or non-target siRNA)-transfected HepG2 cells in RIPA buffer (50 mM Tris-HCl, pH 8.0, 1% Igepal CA-630 (NP-40), 150 mM sodium chloride, 0.5% sodium deoxycholate, and 0.1% sodium dodecyl sulfate). Protein concentrations of the resultant

Molecular Pharmacology Fast Forward. Published on March 28, 2014 as DOI: 10.1124/mol.114.091603
This article has not been copyedited and formatted. The final version may differ from this version.

whole cell lysates were determined using the Bradford Protein Assay (Bio-Rad). 30 µg proteins were separated on SDS-polyacrylamide gels (10%) and transferred to nitrocellulose membranes for western blotting. The anti-UGT2B7 antibody was developed in our laboratory as previously reported (Kerdpin et al. 2009, Hu et al. 2014). The anti-p53 antibody (FL-393) was purchased from Santa Cruz Biotechology (USA). Membranes were incubated first with the primary antibodies and then with a horseradish peroxidase-conjugated donkey anti-rabbit secondary antibody (NeoMarkers). Immunosignals were detected with the SuperSignal®West Pico Chemiluminescent kit (Thermo Fisher Scientific) and an ImageQuant LAS 4000 luminescent image analyser (GE Healthcare). Quantitation of band intensity and background subtraction was performed by Multi Gauge Ver3.0 (FUJIFILM, Japan).

Morphine Glucuronidation assay. HepG2 cells were plated in T75 flasks and cultured until they reached 80% confluence. Cells were then treated with 1 µM EPI or vehicle (0.1% ethanol) for 24 h. Cells were harvested, washed with 1xPBS twice, and then lysed in 250 µl of TE buffer (10 mM Tris-HCl, 1 mM EDTA, pH 7.6), followed by protein concentration determination using the Bradford Protein Assay (Bio-Rad). For morphine glucuronidation assays, duplicate 200 µl reactions of each sample containing 100 mM potassium phosphate pH 7.5, 4 mM MgCl2, 5 mM morphine, 1 mg/ml lysate protein and 5 mM UDPGA, were incubated at 37^{o}C in a shaking water bath for 2 hours. Reactions were terminated by addition of 2 µl $HClO_4$ (70%, v/v). The reaction was cooled on ice for 30 mins and then centrifuged at 10^{o}C at 6,000xg for 10 mins. 10 µl of supernatant fraction of each reaction was subjected to high-performance liquid chromatography (HPLC) analysis using an Agilent 1100 series instrument (Agilent Technologies, Sydney, Australia) as previously reported (Uchaipichat et al. 2011). In brief, retention times for morphine-3-glucuronide, morphine-6-glucuronide, and

Molecular Pharmacology Fast Forward. Published on March 28, 2014 as DOI: 10.1124/mol.114.091603
This article has not been copyedited and formatted. The final version may differ from this version.

morphine were 7.0, 10.3, and 13.6 min, respectively. Concentrations of morphine-3-glucuronide and morphine-6-glucuronide in incubation samples were quantified by comparison of peak areas to those of standard curves prepared over the concentration ranges of 0.5 to 20 and 0.5 to 5 nM, respectively.

Chromatin Immunoprecipitation Assay and Quantitative Real-Time PCR (ChIP-qPCR). ChIP-qPCR was performed as described previously (Hu and Mackenzie 2009). Briefly, HepG2 cells were treated with 1μM EPI, 10 μM nutlin-3α, or vehicle (0.1% ethanol) for 24 h. Cells were then crossed-linked by 1% formadehyde, followed by quenching using 125 mM glycine solution. Cells were lysed, sonicated, and then subjected to immunoprecipitation with 8 μg of the p53 antibody (FL393, Santa Cruz Biotech) or equivalent amounts of the rabbit preimmune IgG control (sc-2027, Santa Cruz Biotech). The resultant chromatin precipitates were captured by Protein A Sepharose CL-4B beads (GE Healthcare, Chalfont St. Giles, UK) and subsequently eluted from the beads in different buffers as described previously (Hu and Mackenzie 2009). Cross-linking was reversed by heating the eluates at 65°C overnight. The resulting DNA/protein precipitates were digested with proteinase K, followed by phenol-chloroform extraction and ethanol precipitation. The DNA pellets were resuspended in 50 μl of Tris-EDTA buffer. Using 2 μl of each of the resultant DNA samples as template, real-time quantitative PCR (qPCR) was performed to quantify the *UGT2B7* promoter region containing the putative p53RE, or the *CYP3A4* promoter region containing a recently reported p53RE as a positive control (Goldstein et al. 2013). As illustrated in Fig. 7A, two promoter regions upstream the *UGT2B7* p53RE were also quantified by qPCR. Data from region 1 served as a negative control, whereas data from region 2 was used to normalize the starting amounts of immunoprecipitated DNA added to each PCR. The p53 binding at the two p53REs and the

Molecular Pharmacology Fast Forward. Published on March 28, 2014 as DOI: 10.1124/mol.114.091603
This article has not been copyedited and formatted. The final version may differ from this version.

negative control region 1 relative to the control region 2 were quantified using the $2^{-\Delta\Delta Ct}$ method (Livak and Schmittgen 2001). qPCR primers are given in Table 1.

Statistical analysis. Statistical analysis was done with a two-tailed Student's t-test using Microsoft Excel 2010. A p value less than 0.05 was considered statistically significant.

Molecular Pharmacology Fast Forward. Published on March 28, 2014 as DOI: 10.1124/mol.114.091603
This article has not been copyedited and formatted. The final version may differ from this version.

Results

Epirubicin Stimulates UGT2B7 mRNA Expression in a Dose-, and Time-dependent Manner in Hepatocellular Carcinoma Cell Lines

Epirubicin (EPI) is genotoxic and inhibits in vitro cell growth (Minotti et al. 2004). EPI concentrations ≤ 1 μM, which are within the EPI plasma and tissular concentration range observed in patients after EPI administration, were used in this study (Italia et al. 1983, Ormrod et al. 1999). To assess potential effects of EPI on *UGT2B7* mRNA levels in a hepatic cellular context, we treated two hepatocellular carcinoma cell lines: namely HepG2 and Huh7, with 1 μM EPI for 24. As shown in Fig. 1, EPI elevated UGT2B7 mRNA levels approximately 23-fold and 6-fold in HepG2 and Huh7 cells, respectively. In contrast, the mRNA levels of UGT2B10 and β-actin (a house-keeping gene) remained unchanged following EPI stimulation. These results indicate that EPI specifically elevated UGT2B7 mRNA levels in HCC cell lines.

Studies with the HepG2 cell line, the most frequently used human liver cell line, have contributed greatly to our understanding of hepatic drug metabolism and detoxification. Given our finding that EPI induced *UGT2B7* expression in HepG2 cells nearly 4 times higher than that in Huh7 cells (Fig. 1), we focused our investigation on HepG2 cells to define the molecular mechanism(s) underlying EPI stimulation of *UGT2B7* expression in a hepatic cellular context. Firstly, we treated HepG2 cells with EPI at 1 μM or lower doses (100, 200, 300, 400, 500, or 800 nM) to define the minimum effective dose. As shown in Fig. 2A, EPI at 200 nM started to elevate *UGT2B7* mRNA levels. This stimulation was gradually increased with increasing doses and at 800 nM reached approximately 30% of that induced by 1 μM. Secondly, we treated HepG2 cells with 1 μM EPI for varying periods (2, 4, 6, 8, 12, or 24 h) to define the minimum effective time. As shown in Fig. 2B, a 2 h-treatment started to

Molecular Pharmacology Fast Forward. Published on March 28, 2014 as DOI: 10.1124/mol.114.091603
This article has not been copyedited and formatted. The final version may differ from this version.

increase UGT2B7 mRNA levels. This stimulation was increased as the length of treatment was extended and at 12 h reached about 50% of the induction as observed at 24 h. Thirdly, we treated HepG2 cells with 1 μM EPI in combination with cycloheximide (2 μM) or actinomycin D (2 μM) for 12 h to determine whether EPI could act at the transcriptional and/or translational levels. As shown in Fig. 2C, the EPI-induced elevation of UGT2B7 mRNA levels was completely abrogated by the transcriptional inhibitor, actinomycin D. This induction was not completely but significantly repressed by the translational inhibitor, cycloheximide, suggesting the necessity for de novo protein synthesis. Taken together, our results indicate that EPI elevates UGT2B7 mRNA levels by stimulating its transcription in a dose- and time-dependent manner in HepG2 cells.

Epirubicin Increases UGT2B7 Protein and Enzymatic Activity

After having demonstrated that EPI elevated UGT2B7 mRNA levels, we prepared whole cell lysates from HepG2 cells treated with 1 μM EPI or vehicle (0.1% ethanol) for 24 h, and then performed Western blotting to see whether EPI could increase UGT2B7 protein levels. Quantitative analysis of the UGT2B7 immuno-signals (Fig 3A) confirmed exposure to 1 μ EPI for 24 h induced UGT2B7 protein levels by 2.7-fold compared to vehicle control (Fig 3B) ($p < 0.05$).

UGT2B7 is the major UGT that conjugates morphine, generating two products: morphine-3-glucuronide and morphine-6-glucuronide (Coffman et al. 1997). We performed glucuronidation assays and subsequent HPLC quantitative analyses to compare morphine-glucuronidating activity between EPI-treated and vehicle-treated HepG2 cells. As shown in Fig. 3C, compared to vehicle-treated cells, EPI-treated HepG2 cells had a significant increase of 5-fold ($p < 0.01$) and 8-fold ($p < 0.01$) in the formation of morphine-3-glucuronide and

Molecular Pharmacology Fast Forward. Published on March 28, 2014 as DOI: 10.1124/mol.114.091603
This article has not been copyedited and formatted. The final version may differ from this version.

morphine-6-glucuronide, respectively. Altogether, these results indicate that EPI increases UGT2B7 protein and enzymatic activity levels in HepG2 cells.

Epirubicin Stimulates the *UGT2B7* Promoter Activity via a Putative p53RE

Having already shown that EPI elevates UGT2B7 mRNA levels through stimulating transcription, we went further to test whether EPI could stimulate *UGT2B7* promoter activity in HepG2 cells. For this purpose, we transfected nine luciferase reporter constructs carrying varying lengths of the *UGT2B7* promoter into HepG2 cells, followed by treatment with 1 μM EPI or vehicle (0.1% ethanol) for 24 h. As shown in Fig. 4A, the activities of *UGT2B7* promoters ≥ 334 bp in length were at least 5-fold higher than those of promoters ≤ 191 bp in vehicle-treated HepG2 cells. EPI stimulation resulted in a significant increase of at least 4-fold in the activity levels of promoters ≥ 334 bp in length; however, this induction was not observed with promoters ≤ 191 bp long. These results suggested that the 143-bp promoter region from nucleotides -191 to -334 harbours a regulatory *cis*-acting element(s), which is critical to both the basal activity of the *UGT2B7* promoter and its response to EPI. To further define the EPI-responsive region, the promoter regions -1 to -240 bp and -1 to -283 bp were amplified from construct 2B7-575/-1 and subsequently cloned into the pGL3-basic vector generating constructs 2B7-240/-1 and 2B7-283/-1. As shown in Fig. 4B, EPI stimulated the activity of construct 2B7-283/-1 but had no impact on the activity of construct 2B7-240/-1. This suggested that the EPI-responsive element(s) resides within the 44-bp promoter region between nucleotides -240 and -283.

As shown in Fig. 4C, bioinformatic analyses of this 44-bp sequence by the LASAGNA program identified a putative p53RE (5'-TGGCATGTCCATACAAGATC-3', core sequences underlined) between nucleotides -251 and -270 (Lee and Huang 2013). In addition, this 44-bp region also contains a Farnesoid X receptor (FXR) binding site (5'-

Molecular Pharmacology Fast Forward. Published on March 28, 2014 as DOI: 10.1124/mol.114.091603
This article has not been copyedited and formatted. The final version may differ from this version.

GATCCTTGATATTAG-3') between nucleotides -239 and -254, which has been shown to be involved in repressing *UGT2B7* expression by lithocholic acid in CaCo-2 cells (Lu et al. 2005). Of interest, there is a 4-bp overlap between this FXR site and our predicted p53RE. The strongest p53REs, such as the *p21* p53-RE2, usually have no spacer between two decamers (RRRCWWGYYY) (Riley et al. 2008, Saramaki et al. 2006). The CWWG core sequence in the form of CATG is associated with higher binding affinity compared to the three other possible sequences (CAAG, CTAG, or CTTG) (Menendez et al. 2009). The *UGT2B7* p53RE has no spacer between the two 10-base decamers and has the strongest core sequence of CATG at the 5' decamer. Based on these observations, the putative *UGT2B7* p53RE is a highly conserved p53RE.

To identify the EPI-responsive sequence, we mutated this 44-bp region in the -575/-1 promoter context at five positions generating five mutated reporter constructs (termed 2B7-575/-1/MT1-5). As shown in Fig. 4C, there was a 4-bp change in each mutation. Mutants MT1 and MT2 did not alter the p53RE and FXR site sequences. MT3 changed the core sequence of CATG at the 5' half-site to AGTG (mutated bases underlined), whereas MT4 mutated the core sequence of CAAG at the 3' half-site to AAAG. In addition to these changes, MT3 and MT4 mutated another 2-3 bases immediately 5' to the core sequences. MT5 changed 4 bases at the FXR site (5'-GATCCTTGATACGGT-3', mutated bases underlined). We transfected these mutants into HepG2 cells to see whether they could affect EPI-responsiveness. As shown in Fig. 4B, two mutations (MT3 and MT4) which altered the p53RE site, completely abolished the capacity of EPI to stimulate promoter activity. In contrast, the remaining three mutations that mutated the FXR site or sequences upstream of the p53RE had no impact on the EPI-induced *UGT2B7* promoter activity. Interestingly, the mutation in the FXR site (MT5) slightly enhanced promoter activity, suggesting that inhibitory effects of FXR on the *UGT2B7* promoter were disrupted. FXR has been reported to

Molecular Pharmacology Fast Forward. Published on March 28, 2014 as DOI: 10.1124/mol.114.091603
This article has not been copyedited and formatted. The final version may differ from this version.

inhibit UGT2B7 expression in Caco-2 cells exposed to lithocholic acid (Lu et al. 2005). Collectively, these data indicate that EPI induces *UGT2B7* promoter activity through the p53RE in its proximal promoter.

siRNA-mediated Knockdown of p53 Reduces the Capacity of Epirubicin to Stimulate UGT2B7 Gene Expression

Having already demonstrated that EPI stimulates *UGT2B7* promoter activity via the p53RE, we transfected HepG2 cells with anti-p53 siRNAs to knockdown p53 protein levels to see whether this could repress the capacity of EPI to induce *UGT2B7* expression. As shown in Fig. 5A, the anti-p53 siRNA specifically reduced p53 protein levels to approximately 30% of that in non-target siRNA transfected cells ($p < 0.01$). *p21* (encoding cyclin-dependent kinase inhibitor 1A) and *CYP3A4* (encoding cytochrome P450, family 3, subfamily A, polypeptide 4) are p53 target genes (el-Deiry et al. 1993, Goldstein et al. 2013). As shown in Fig. 5B, siRNA-mediated knockdown of p53 expression significantly reduced the induction of EPI on the two p53 target genes (*p21* and *CYP3A4*) as well as *UGT2B7*, but had no impact on *UGT2B10*, whose mRNA levels were not elevated by EPI. EPI did not activate PXR in HepG2 cells (data not shown), in agreement with studies showing that overexpression of all three PXR variants does not stimulate *UGT2B7* expression (Gardner-Stephen et al. 2004) and that rifampin, an agonist of PXR, has no effect on *UGT2B7* promoter activity in HepG2 cells (Jeong et al. 2008). Taken together, these data provide direct evidence for an involvement of p53 in the induction of *UGT2B7* expression by EPI. This was further supported by the demonstration that there was a strict correlation between the dose- and time-dependent induction of UGT2B7 by EPI (Fig. 2) and p53 protein levels (Supplemental Fig. 1).

Molecular Pharmacology Fast Forward. Published on March 28, 2014 as DOI: 10.1124/mol.114.091603
This article has not been copyedited and formatted. The final version may differ from this version.

The p53 Activator Nutlin-3α Stimulates *UGT2B7* Gene Expression

The stability and transcriptional activity of the p53 protein are negatively regulated by its binding to MDM2 (mouse double minute 2 homolog) (Michael and Oren 2003). Nutlin-3α is a MDM2 antagonist and its binding to MDM2 disrupts its interaction with p53 (Vassilev et al. 2004). This disassociation stabilizes p53 protein resulting in its accumulation in the nuclei, thus activating the p53 pathway (Menendez et al. 2009, Riley et al. 2008). We treated HepG2 cells with nutlin-3α to see whether this agent could stimulate *UGT2B7* expression. For this purpose, we treated HepG2 cells with nutlin-3α at 10 μM for 24 h and then performed RT-qPCR to measure target mRNA levels. The choice of 10 μM nutlin-3α was in line with previous similar cell-based studies (Goldstein et al. 2013). As expected, nutlin-3α stimulated *p21* expression *(*$p < 0.01$) and did not affect *UGT2B10* expression (Fig. 6A). Nutlin-3α significantly increased *UGT2B7* expression ($p < 0.01$), thus verifying *UGT2B7* as a p53 target gene. To further confirm that nutlin-3α stimulates *UGT2B7* expression through the p53-pathway, we transfected HepG2 cells with anti-p53 siRNAs to reduce p53 protein levels prior to nutlin-3α stimulation. As shown in Fig. 6B, the nutlin-3α-induced mRNA levels of *p21* and *UGT2B7* in anti-p53 siRNA-transfected cells were only 5% and 18%, respectively, of that in non-target siRNA-transfected cells. *UGT2B10* was not induced by nutlin-3α, and as a result its mRNA levels remained at similar levels in these experiments. Collectively, these data reinforced our notion of *UGT2B7* as a novel p53 target gene in HepG2 cells.

p53 is Recruited to the *UGT2B7* p53 Site in HepG2 Cells in Response to Epirubicin

Chromatin immunoprecipitation followed by quantitative real-time PCR (ChIP-qPCR) was performed to see whether endogenous p53 proteins could bind to the *UGT2B7* p53RE in HepG2 cells following stimulation with EPI or nutlin-3α. ChIP assays were performed with an anti-p53 antibody and the rabbit preimmune IgG control for normalizing against possible

Molecular Pharmacology Fast Forward. Published on March 28, 2014 as DOI: 10.1124/mol.114.091603
This article has not been copyedited and formatted. The final version may differ from this version.

nonselective background immunoprecipitation. For this purpose, HepG2 cells were treated with 1 μM EPI, 10 μM nutlin-3α, or vehicle (0.1% ethanol) for 24 h and then subjected to ChIP-qPCR. As shown in Fig. 7A, three *UGT2B7* promoter regions were quantified from immunoprecipitated samples, including the p53RE-containing region (-355/-209) and two control regions (-3026/-2907 and -7906/-7747). Data from Control region 1 served as a negative control, whereas data from Control region 2 were used for normalization of starting amounts of DNA amplified in different samples. For a positive control, the promoter region containing the *CYP3A4* p53 site, which was recently shown to be bound by p53 in nutlin-3α-treated HepG2 cells (Goldstein et al. 2013), was also quantified. As shown in Fig. 7B, the binding of p53 to the *CYP3A4* p53RE was increased by 2.7-fold ($p < 0.05$) and 3-fold ($p < 0.05$) following stimulation with EPI and nutlin-3α, respectively, compared to controls precipitated by equivalent amounts of the irrelevant preimmune-IgG serum (designated as IgG) (Fig. 7B). In agreement with our hypothesis, EPI and nutlin-3α increased p53 binding at the *UGT2B7* p53RE 6.5-fold ($p < 0.01$) and 3.7-fold ($p < 0.01$), respectively. In contrast, neither EPI nor nutlin-3α enhanced p53 binding at the negative Control region 1, which is about 3 kb upstream of the p53RE. Taken together, these data clearly demonstrated that p53 is recruited to the *UGT2B7* p53RE following EPI stimulation.

Molecular Pharmacology Fast Forward. Published on March 28, 2014 as DOI: 10.1124/mol.114.091603
This article has not been copyedited and formatted. The final version may differ from this version.

Discussion

In the present study, we identified a functional p53RE in the *UGT2B7* proximal promoter that highly resembles the p53RE consensus sequence (Menendez et al. 2009, Riley et al. 2008). We demonstrated that EPI stimulated *UGT2B7* promoter activity via this p53RE and enhanced in vivo p53 binding at this site in the hepatic HepG2 cell line. Knockdown of p53 expression by siRNA silencing technology significantly repressed the capacity of EPI to induce *UGT2B7* transcription. We further showed that the p53 activator nutlin-3α stimulated *UGT2B7* expression and recruited p53 protein to the UGT2B7 p53RE in HepG2 cells. Collectively, these data indicate that *UGT2B7* is a novel p53 target gene. This finding is consistent with the important role of p53 in maintaining genome stability upon exposure to genotoxic agents, such as anthracyclines (Horn and Vousden 2007).

It is well-established that p53 is activated in target cancer cells by genotoxic agents including anthracyclines (Mansilla, Pina and Portugal 2003, Tishler et al. 1993). Anthracyclines mainly act as DNA intercalators and topoisomerase II inhibitors to achieve their anticancer activities (Minotti et al. 2004). The intercalation of anthracyclines into DNA prohibits DNA replication and RNA transcription. Inhibition of topoisomerase II activity stabilizes the anthracycline-DNA-topisomerase II ternary complex and prohibits the resealing of the DNA double helix during DNA replication and RNA transcription. This ultimately leads to DNA damage (Cortes-Funes and Coronado 2007). The rate of damage to DNA depends on the dose of the genotoxic agent and time of exposure. The lag in UGT2B7 induction over the first 8 hr and with lower doses of EPI most likely reflects the time required for generation of EPI-induced DNA damage and elevation in p53 levels [supplemental Fig. 1].

Molecular Pharmacology Fast Forward. Published on March 28, 2014 as DOI: 10.1124/mol.114.091603
This article has not been copyedited and formatted. The final version may differ from this version.

The accumulation of DNA damage in the nuclei triggers the p53-mediated DNA damage response pathway (Horn and Vousden 2007, Mansilla et al. 2003, Tishler et al. 1993, Menendez et al. 2009, Riley et al. 2008). Through this pathway, p53 activates transcription of downstream targets that mainly belong to two sets of genes. The first set is involved in cell cycle arrest and DNA repair and allows repair if the damage is mild. The second set of genes is involved in apoptosis, leading to cell death if DNA damage is severe and beyond repair. Our finding of EPI-induced *UGT2B7* expression indicates that drug-metabolizing enzymes may represent a novel third set of genes that are mobilized by the p53-mediated response pathway to promote removal of genotoxic agents from target cancer cells. This hypothesis is supported by recent observations that multiple CYPs including *CYP3A4* are p53 target genes (Goldstein et al. 2013). Genotoxic anticancer drugs (e.g. DOX) increased CYP3A4 expression and enzymatic activity in HepG2 cells (Goldstein et al. 2013). We confirmed this finding (data not shown) and further demonstrated that similar to DOX, EPI enhanced *CYP3A4* transcription via the p53 pathway in HepG2 cells.

Hepatocellular carcinoma (HCC) ranks the fifth most frequent cancer and the third leading cause of cancer-related death worldwide (Lin, Hoffmann and Schemmer 2012). Chemotherapy is the only treatment option for patients with non-resectable advanced HCC (Lin et al. 2012). DOX and EPI are among the most commonly used chemotherapeutic drugs against HCC (Marelli et al. 2007). To enhance efficacy and reduce systemic toxicity, anthracyclines are usually given by intrahepatic arterial infusion for treating HCC (Marelli et al. 2007). EPI has been administered alone (monotherapy), in combination with mitomycin or cisplatin (double therapy), or together with mitomycin and cisplatin (triple therapy) (Marelli et al. 2007). Due to intrinsic resistance, these EPI-containing regimens achieve only a 10-25% response rate and rapidly lead to treatment failure (acquired resistance) (Lin et al. 2012). Resistance to anthracyclines is not well understood and may be as a result of 1) changes in

Molecular Pharmacology Fast Forward. Published on March 28, 2014 as DOI: 10.1124/mol.114.091603
This article has not been copyedited and formatted. The final version may differ from this version.

the expression of uptake (e.g OATP1B1) and efflux (e.g. p-glycoprotein) transporters, 2) modifications in apoptosis machinery, and 3) altered topoisomerase II activity (Piekarski and Jelinska 2013). Our results from the present study suggest that upregulation of *UGT2B7* by EPI in HCC cancer cells might partly contribute to acquired resistance to the above mentioned EPI-based HCC chemotherapy. Cisplatin, a genotoxic anticancer drug, is listed as a CYP3A4/5 substrate (Harmsen et al. 2007). Cisplatin has been recently shown to be able to stimulate *CYP3A4* expression in HepG2 cells (Goldstein et al. 2013). This facilitates detoxification of cisplatin itself within liver cancer cells. This observation combined with our finding of induction of *CYP3A4* by EPI in HepG2 cells suggests that enhanced CYP3A4 activity might play a role in the development of resistance to EPI/cisplatin-containing HCC chemotherapy. In addition to HCC, EPI is used in the treatment of various non-hepatic cancers (e.g. lung, stomach, and bladder carcinomas) that originate from tissues in which *UGT2B7* is expressed (Nakamura et al. 2008b). Whether EPI could also stimulate *UGT2B7* expression in non-hepatic cancer cellular contexts warrants further investigation. A recent study has shown that EPI was able to stimulate *UGT2B7* expression in Melanoma cancer cells (Dellinger et al. 2012). However, the molecular mechanism(s) underlying this regulation remained undefined in this study. As melanoma is resistant to anthracyclines and EPI is not usually used in the treatment of melanoma, the clinical significance of this finding is not clear.

Regulation of *UGT*s by their substrates (or metabolites) has been frequently reported. Regulation of a *UGT* by a drug that is primarily metabolized by this UGT may be relevant to therapeutic efficacy, resistance, or toxicity of this drug. Irinotecan, a DNA isomerase I inhibitor, is the first-line anticancer drug for metastatic colorectal cancer. The active metabolite 7-ethyl-10-hydroxylcamptothecin (SN-38) of irinotecan is primarily inactivated by UGT1A1. Studies have shown that overexpression of UGT1A1 in a lung cancer cell line (PC-7/CPT) (Oguri et al. 2004) or induction of *UGT1A1* by SN-38 in colon (LS180) and liver

Molecular Pharmacology Fast Forward. Published on March 28, 2014 as DOI: 10.1124/mol.114.091603
This article has not been copyedited and formatted. The final version may differ from this version.

(HepG2) cancer cell lines is associated with irinotecan resistance (Basseville et al. 2011). The induction of *UGT2B7* by its substrate EPI described in the present study, may represent a new example of this type of regulation.

The better tolerability and less cardiotoxicity of EPI compared to other classic anthracyclines has been attributed to its unique hepatic glucuronidation metabolic pathway (Ormrod et al. 1999). This hypothesis is now further supported by our finding that EPI upregulates its own detoxifying gene *UGT2B7* in a hepatic cellular context. EPI is administered intravenously in the treatment of non-hepatic cancers (Minotti et al. 2004). After administration, EPI is rapidly distributed into human tissues (Minotti et al. 2004). Early studies have shown that after administration of 10 mg/m^2 of EPI to patents within 2-4 h prior to surgery, the concentration of EPI in liver metastases was 996 ng/g (Italia et al. 1983). This estimate is similar to the maximum EPI concentration of 1 μM used in the present study. The concentration of EPI in liver tissues is expected to be higher than this estimate after therapeutic doses of EPI (60-135 mg/m^2) (Minotti et al. 2004). Our finding that EPI enhanced *UGT2B7* expression and activity in a hepatic cellular context at therapeutic relevant doses suggests that for treating non-hepatic cancers, EPI may be able to promote its own hepatic systemic clearance. This capacity of EPI to enhance its own systemic clearance could reduce therapeutic efficacy or even contribute to development of acquired resistance to EPI-containing chemotherapy. These hypotheses await further validation clinically and experimentally using other hepatic models such as primary hepatocytes and transgenic mice (Yueh, Mellon and Tukey 2011).

In addition to EPI, UGT2B7 is involved in the glucuronidation of a variety of endobiotics and xenobiotics, including bile acids, steroid hormones, fatty acids, retinoids, non-steroidal anti-inflammatory drugs, and morphine (Radominska-Pandya, Little and Czernik 2001). *UGT2B7* is expressed in the liver and the gastrointestinal tract (Nakamura et

Molecular Pharmacology Fast Forward. Published on March 28, 2014 as DOI: 10.1124/mol.114.091603
This article has not been copyedited and formatted. The final version may differ from this version.

al. 2008b, Ohno and Nakajin 2009, Izukawa et al. 2009, Tukey and Strassburg 2001). Regulation of hepatic and gastrointestinal *UGT2B7* expression is thus critical for its substrate detoxification and clearance. Regulation of *UGT2B7* has been investigated using liver and colon cancer cell lines and transgenic mice. The transcription factors known to regulate *UGT2B7* and their relevant cis-activating elements at its proximal promoter are summarized in Fig. 8 (Gregory et al. 2006, Ishii et al. 2000, Lu et al. 2005, Nakamura et al. 2008a, Yueh et al. 2011). Our identification of *UGT2B7* as a novel p53 target gene provides new insights into the mechanisms controlling hepatic *UGT2B7* expression.

In conclusion, this study demonstrates that EPI upregulates its own detoxifying enzyme UGT2B7 via the p53-mediated pathway. This regulation may contribute to the development of tumour resistance to EPI-containing HCC chemotherapy and may also provide a new explanation for the better pharmacological profiles of EPI compared to other anthracyclines. Combined with the recently described p53-mediated induction of CYP enzymes by genotoxic agents in HCC cell lines (Goldstein et al. 2013), our finding further suggests that genotoxic agent-detoxifying genes may represent a novel group of genes that are activated by the p53-mediated response pathway to clear genotoxic agents locally from the tumour site, or possibly systemically from the body through the liver. This decreases chemotherapeutic efficacy and may lead to tumour resistance to genotoxic anticancer drugs.

Molecular Pharmacology Fast Forward. Published on March 28, 2014 as DOI: 10.1124/mol.114.091603
This article has not been copyedited and formatted. The final version may differ from this version.

Authorship Contributions

Participated in research design: Hu and Mackenzie

Conducted experiments: Hu and Rogers

Performed data analysis: Hu and Mackenzie

Wrote or contributed to the writing of the manuscript: Hu and Mackenzie

Molecular Pharmacology Fast Forward. Published on March 28, 2014 as DOI: 10.1124/mol.114.091603
This article has not been copyedited and formatted. The final version may differ from this version.

References

Bains, O. S., M. J. Karkling, T. A. Grigliatti, R. E. Reid & K. W. Riggs (2009) Two nonsynonymous single nucleotide polymorphisms of human carbonyl reductase 1 demonstrate reduced in vitro metabolism of daunorubicin and doxorubicin. *Drug Metab Dispos,* 37**,** 1107-1114.

Basseville, A., L. Preisser, S. de Carne Trecesson, M. Boisdron-Celle, E. Gamelin, O. Coqueret & A. Morel (2011) Irinotecan induces steroid and xenobiotic receptor (SXR) signaling to detoxification pathway in colon cancer cells. *Mol Cancer,* 10**,** 80.

Coffman, B. L., G. R. Rios, C. D. King & T. R. Tephly (1997) Human UGT2B7 catalyzes morphine glucuronidation. *Drug Metab Dispos,* 25**,** 1-4.

Congiu, M., M. L. Mashford, J. L. Slavin & P. V. Desmond (2002) UDP glucuronosyltransferase mRNA levels in human liver disease. *Drug Metab Dispos,* 30**,** 129-134.

Cortes-Funes, H. & C. Coronado (2007) Role of anthracyclines in the era of targeted therapy. *Cardiovasc Toxicol,* 7**,** 56-60.

Dellinger, R. W., H. H. Matundan, A. S. Ahmed, P. H. Duong & F. L. Meyskens, Jr. (2012) Anti-cancer drugs elicit re-expression of UDP-glucuronosyltransferases in melanoma cells. *PLoS One,* 7**,** e47696.

el-Deiry, W. S., T. Tokino, V. E. Velculescu, D. B. Levy, R. Parsons, J. M. Trent, D. Lin, W. E. Mercer, K. W. Kinzler & B. Vogelstein (1993) WAF1, a potential mediator of p53 tumor suppression. *Cell,* 75**,** 817-825.

Gardner-Stephen, D., J. M. Heydel, A. Goyal, Y. Lu, W. Xie, T. Lindblom, P. Mackenzie & A. Radominska-Pandya (2004) Human PXR variants and their differential effects on the regulation of human UDP-glucuronosyltransferase gene expression. *Drug Metab Dispos,* 32**,** 340-347.

Molecular Pharmacology Fast Forward. Published on March 28, 2014 as DOI: 10.1124/mol.114.091603
This article has not been copyedited and formatted. The final version may differ from this version.

Goldstein, I., N. Rivlin, O. Y. Shoshana, O. Ezra, S. Madar, N. Goldfinger & V. Rotter (2013) Chemotherapeutic agents induce the expression and activity of their clearing enzyme CYP3A4 by activating p53. *Carcinogenesis,* 34**,** 190-198.

Gregory, P. A., D. A. Gardner-Stephen, A. Rogers, M. Z. Michael & P. I. Mackenzie (2006) The caudal-related homeodomain protein Cdx2 and hepatocyte nuclear factor 1alpha cooperatively regulate the UDP-glucuronosyltransferase 2B7 gene promoter. *Pharmacogenet Genomics,* 16**,** 527-536.

Harmsen, S., I. Meijerman, J. H. Beijnen & J. H. Schellens (2007) The role of nuclear receptors in pharmacokinetic drug-drug interactions in oncology. *Cancer Treat Rev,* 33**,** 369-380.

Horn, H. F. & K. H. Vousden (2007) Coping with stress: multiple ways to activate p53. *Oncogene,* 26**,** 1306-1316.

Hu, D. G., D. Gardner-Stephen, G. Severi, P. A. Gregory, J. Treloar, G. G. Giles, D. R. English, J. L. Hopper, W. D. Tilley & P. I. Mackenzie (2010) A novel polymorphism in a forkhead box A1 (FOXA1) binding site of the human UDP glucuronosyltransferase 2B17 gene modulates promoter activity and is associated with altered levels of circulating androstane-3alpha,17beta-diol glucuronide. *Mol Pharmacol,* 78**,** 714-722.

Hu, D. G. & P. I. Mackenzie (2009) Estrogen receptor alpha, fos-related antigen-2, and c-Jun coordinately regulate human UDP glucuronosyltransferase 2B15 and 2B17 expression in response to 17beta-estradiol in MCF-7 cells. *Mol Pharmacol,* 76**,** 425-439.

Hu, D. G. & P. I. Mackenzie (2010) Forkhead box protein A1 regulates UDP-glucuronosyltransferase 2B15 gene transcription in LNCaP prostate cancer cells. *Drug Metab Dispos,* 38**,** 2105-2109.

Hu, D. G., R. Meech, L. Lu, R. A. McKinnon & P. I. Mackenzie (2014) Polymorphisms and Haplotypes of the UDP-Glucuronosyltransferase 2B7 Gene Promoter. *Drug Metab Dispos*. doi:10.1124/dmd.113.056630.

Innocenti, F., L. Iyer, J. Ramirez, M. D. Green & M. J. Ratain (2001) Epirubicin glucuronidation is catalyzed by human UDP-glucuronosyltransferase 2B7. *Drug Metab Dispos,* 29**,** 686-692.

Ishii, Y., A. J. Hansen & P. I. Mackenzie (2000) Octamer transcription factor-1 enhances hepatic nuclear factor-1alpha-mediated activation of the human UDP glucuronosyltransferase 2B7 promoter. *Mol Pharmacol,* 57**,** 940-947.

Italia, C., L. Paglia, A. Trabattoni, S. Luchini, F. Villas, L. Beretta, G. Marelli & N. Natale (1983) Distribution of 4'epi-doxorubicin in human tissues. *Br J Cancer,* 47**,** 545-547.

Izukawa, T., M. Nakajima, R. Fujiwara, H. Yamanaka, T. Fukami, M. Takamiya, Y. Aoki, S. Ikushiro, T. Sakaki & T. Yokoi (2009) Quantitative analysis of UDP-glucuronosyltransferase (UGT) 1A and UGT2B expression levels in human livers. *Drug Metab Dispos,* 37**,** 1759-1768.

Jeong, H., S. Choi, J. W. Song, H. Chen & J. H. Fischer (2008) Regulation of UDP-glucuronosyltransferase (UGT) 1A1 by progesterone and its impact on labetalol elimination. Xenobiotica, 38, 62-75.

Jin, Y. & T. M. Penning (2007) Aldo-keto reductases and bioactivation/detoxication. *Annu Rev Pharmacol Toxicol,* 47**,** 263-292.

Kerdpin, O., P. I. Mackenzie, K. Bowalgaha, M. Finel & J. O. Miners (2009) Influence of N-terminal domain histidine and proline residues on the substrate selectivities of human UDP-glucuronosyltransferase 1A1, 1A6, 1A9, 2B7, and 2B10. *Drug Metab Dispos,* 37**,** 1948-1955.

Le Bot, M. A., J. M. Begue, D. Kernaleguen, J. Robert, D. Ratanasavanh, J. Airiau, C. Riche & A. Guillouzo (1988) Different cytotoxicity and metabolism of doxorubicin, daunorubicin, epirubicin, esorubicin and idarubicin in cultured human and rat hepatocytes. *Biochem Pharmacol,* 37**,** 3877-3887.

Lee, C. & C. H. Huang (2013) LASAGNA-Search: an integrated web tool for transcription factor binding site search and visualization. *Biotechniques,* 54**,** 141-153.

Lin, S., K. Hoffmann & P. Schemmer (2012) Treatment of Hepatocellular Carcinoma: A Systematic Review. *Liver Cancer,* 1**,** 144-158.

Livak, K. J. & T. D. Schmittgen (2001) Analysis of relative gene expression data using real-time quantitative PCR and the 2(-Delta Delta C(T)) Method. *Methods,* 25**,** 402-408.

Lu, Y., J. M. Heydel, X. Li, S. Bratton, T. Lindblom & A. Radominska-Pandya (2005) Lithocholic acid decreases expression of UGT2B7 in Caco-2 cells: a potential role for a negative farnesoid X receptor response element. *Drug Metab Dispos,* 33**,** 937-946.

Mackenzie, P. I., K. W. Bock, B. Burchell, C. Guillemette, S. Ikushiro, T. Iyanagi, J. O. Miners, I. S. Owens & D. W. Nebert (2005) Nomenclature update for the mammalian UDP glycosyltransferase (UGT) gene superfamily. *Pharmacogenet Genomics,* 15**,** 677-685.

Mackenzie, P. I., I. S. Owens, B. Burchell, K. W. Bock, A. Bairoch, A. Belanger, S. Fournel-Gigleux, M. Green, D. W. Hum, T. Iyanagi, D. Lancet, P. Louisot, J. Magdalou, J. R. Chowdhury, J. K. Ritter, H. Schachter, T. R. Tephly, K. F. Tipton & D. W. Nebert (1997) The UDP glycosyltransferase gene superfamily: recommended nomenclature update based on evolutionary divergence. *Pharmacogenetics,* 7**,** 255-269.

Mansilla, S., B. Pina & J. Portugal (2003) Daunorubicin-induced variations in gene transcription: commitment to proliferation arrest, senescence and apoptosis. *Biochem J,* 372**,** 703-711.

Marelli, L., R. Stigliano, C. Triantos, M. Senzolo, E. Cholongitas, N. Davies, J. Tibballs, T. Meyer, D. W. Patch & A. K. Burroughs (2007) Transarterial therapy for hepatocellular carcinoma: which technique is more effective? A systematic review of cohort and randomized studies. *Cardiovasc Intervent Radiol,* 30**,** 6-25.

Menendez, D., A. Inga & M. A. Resnick (2009) The expanding universe of p53 targets. *Nat Rev Cancer,* 9**,** 724-737.

Michael, D. & M. Oren (2003) The p53-Mdm2 module and the ubiquitin system. *Semin Cancer Biol,* 13**,** 49-58.

Minotti, G., P. Menna, E. Salvatorelli, G. Cairo & L. Gianni (2004) Anthracyclines: molecular advances and pharmacologic developments in antitumor activity and cardiotoxicity. *Pharmacol Rev,* 56**,** 185-229.

Nakamura, A., M. Nakajima, E. Higashi, H. Yamanaka & T. Yokoi (2008a) Genetic polymorphisms in the 5'-flanking region of human UDP-glucuronosyltransferase 2B7 affect the Nrf2-dependent transcriptional regulation. *Pharmacogenet Genomics,* 18**,** 709-720.

Nakamura, A., M. Nakajima, H. Yamanaka, R. Fujiwara & T. Yokoi (2008b) Expression of UGT1A and UGT2B mRNA in human normal tissues and various cell lines. *Drug Metab Dispos,* 36**,** 1461-1464.

Oguri, T., T. Takahashi, M. Miyazaki, T. Isobe, N. Kohno, P. I. Mackenzie & Y. Fujiwara (2004) UGT1A10 is responsible for SN-38 glucuronidation and its expression in human lung cancers. *Anticancer Res,* 24**,** 2893-2896.

Ohno, S. & S. Nakajin (2009) Determination of mRNA expression of human UDP-glucuronosyltransferases and application for localization in various human tissues by real-time reverse transcriptase-polymerase chain reaction. *Drug Metab Dispos,* 37**,** 32-40.

Ormrod, D., K. Holm, K. Goa & C. Spencer (1999) Epirubicin: a review of its efficacy as adjuvant therapy and in the treatment of metastatic disease in breast cancer. *Drugs Aging,* 15**,** 389-416.

Piekarski, M. & A. Jelinska (2013) Anthracyclines still prove effective in anticancer therapy. *Mini Rev Med Chem,* 13**,** 627-634.

Radominska-Pandya, A., J. M. Little & P. J. Czernik (2001) Human UDP-glucuronosyltransferase 2B7. *Curr Drug Metab,* 2**,** 283-298.

Riley, T., E. Sontag, P. Chen & A. Levine (2008) Transcriptional control of human p53-regulated genes. *Nat Rev Mol Cell Biol,* 9**,** 402-412.

Saramaki, A., C. M. Banwell, M. J. Campbell & C. Carlberg (2006) Regulation of the human p21(waf1/cip1) gene promoter via multiple binding sites for p53 and the vitamin D3 receptor. *Nucleic Acids Res,* 34**,** 543-554.

Tishler, R. B., S. K. Calderwood, C. N. Coleman & B. D. Price (1993) Increases in sequence specific DNA binding by p53 following treatment with chemotherapeutic and DNA damaging agents. *Cancer Res,* 53**,** 2212-2216.

Tukey, R. H. & C. P. Strassburg (2001) Genetic multiplicity of the human UDP-glucuronosyltransferases and regulation in the gastrointestinal tract. *Mol Pharmacol,* 59**,** 405-414.

Uchaipichat, V., P. Raungrut, N. Chau, B. Janchawee, A. M. Evans & J. O. Miners (2011) Effects of ketamine on human UDP-glucuronosyltransferases in vitro predict potential drug-drug interactions arising from ketamine inhibition of codeine and morphine glucuronidation. *Drug Metab Dispos,* 39**,** 1324-1328.

Vassilev, L. T., B. T. Vu, B. Graves, D. Carvajal, F. Podlaski, Z. Filipovic, N. Kong, U. Kammlott, C. Lukacs, C. Klein, N. Fotouhi & E. A. Liu (2004) In vivo activation of the p53 pathway by small-molecule antagonists of MDM2. *Science,* 303**,** 844-848.

Yueh, M. F., P. L. Mellon & R. H. Tukey (2011) Inhibition of human UGT2B7 gene expression in transgenic mice by the constitutive androstane receptor. *Mol Pharmacol*, 79**,** 1053-1060.

Footnote

This work was supported by the National Health and Medical Research Council (NHMRC) of Australia [grant APP1020931]. PIM is a NHMRC Senior Principal Research Fellow.

Molecular Pharmacology Fast Forward. Published on March 28, 2014 as DOI: 10.1124/mol.114.091603
This article has not been copyedited and formatted. The final version may differ from this version.

Figure legends

Figure 1. Epirubicin elevates UGTB7 mRNA levels in hepatocellular carcinoma HepG2 and Huh7 cell lines. HepG2 or Huh7 cells were plated in 6-well plates and cultured for 2-3 days until they reached approximately 80% confluence. Cells were then treated in triplicate with 1 μM EPI or vehicle (0.1% ethanol) for 24 h. Total RNA was extracted and reverse-transcribed to generate cDNA, followed by quantitative real-time PCR to quantify the mRNA levels of three genes (*UGT2B7*, *UGT2B10*, and *β-actin*) as described under *Materials and Methods*. Data are presented as fold-induction in target gene mRNA levels in EPI-treated cells over those (set as value of 1) in vehicle-treated cells. Data shown are means ± 1 S.D. from a representative experiment of three independent experiements performed in triplicate. * $p < 0.05$, ** $p < 0.01$

Figure 2. Epirubicin stimulates *UGT2B7* transcription in a time- and dose-dependent manner in HepG2 cells. A: HepG2 cells were treated with vehicle (0.1% ethanol) or various concentrations of EPI (100, 200, 300, 400, 500, 800, or 1000 nM) for 24 h. B: cells were treated with 1 μM EPI for 2, 4, 6, 8, 12, or 24 h. C: HepG2 cells were treated with vehicle (0.1% ethanol), 2 μM actinomycin D (ATD), 2 μM cycloheximide (CHX), 1 μM EPI, or a combination of 1 μM EPI with 2 μM CHX or 2 μM ATD for 12 h. After treatment, total RNA was extracted from cells and reverse-transcribed to generate cDNA, followed by quantitative real-time PCR to quantify the mRNA levels of *UGT2B7* and *UGT2B10* as described under *Materials and Methods*. Data presented as fold change of each target mRNA levels in cells that were treated as indicated compared to those (set as a value of 1) in vehicle-treated cells. Data shown are means ± 1 S.D. from a representative experiment of two independent experiments performed in triplicate. ** $p < 0.01$.

Molecular Pharmacology Fast Forward. Published on March 28, 2014 as DOI: 10.1124/mol.114.091603
This article has not been copyedited and formatted. The final version may differ from this version.

Figure 3. Epirubicin increases UGT2B7 protein levels and enzymatic activity in HepG2 cells. A: cells were treated with 1 μM EPI or vehicle (0.1% ethanol) for 24 h in triplicate. After treatment, cells were harvested for preparing whole cell lysate. Whole cell lysates were also prepared from wild type HEK293 cells that expressed no UGT2B7 proteins for a negative control or HEK293 cells that stably expressed UGT2B7 proteins for a positive control. 30 μg proteins of whole cell lysates were subjected to western blotting using an antibody against UGT2B7 (top) or β-actin (bottom) as described in *Materials and Methods*. B: shown is fold-induction of UGT2B7 protein levels in EPI-treated cells compared to that (set a value of 1) in vehicle-treated cells. C: Morphine glucuronidation assays were performed using cell lysates from EPI-treated or vehicle-treated HepG2 cells as described in *Materials and Methods*. Shown are fold-changes in the formation of morphine-3-glucuronide (morphine-3-G) or morphine-6-glucuronide (morphine-6-G) in EPI-treated cells compared to that (set as a value of 1) in vehicle-treated HepG2 cells. * $p < 0.05$, ** $p < 0.01$

Figure 4. Deletion and mutagenesis analyses of the *UGT27* promoter in HepG2 cells identify a p53 response element (p53RE) that mediates epirubicin responsiveness. A and B: a series of deleted (A) and mutated (B) *UGT2B7* promoter constructs were transfected into HepG2 cells. Briefly, cells were plated into 96-well plates and cultured until they reached 70% confluence. Cells were transfected in triplicate with 100 ng of each promoter construct, 8 ng of PRL-null vector, and 0.8 ul of Lipofectamine 2000. 24 h after transfection, transfection medium was removed and replaced with fresh medium. 48 h after transfection, cells were treated with 1 μM EPI or vehicle (0.1% ethanol) for 24 h. After treatment, cells were harvested and assayed for firefly luciferase activity as described under *Materials and Methods*. After normalized to that of the promoter-less pGL3-basic vector, data was

Molecular Pharmacology Fast Forward. Published on March 28, 2014 as DOI: 10.1124/mol.114.091603
This article has not been copyedited and formatted. The final version may differ from this version.

presented as fold induction of the activities of promoter constructs in EPI-treated cells compared to that (set at a value of 1) in vehicle-treated cells. Data shown are means ± 1 S. D. from a representative experiment of three independent experiments performed in triplicate. C: shown are five mutations at the *UGT2B7* promoter between nucleotides -288 and -238 that mutated the p53RE (MT3 and MT4), FXR site (MT5), or sequences that are upstream of the p53RE (MT1 and MT2). Mutated sequences are boxed with the wild type sequences underlined and the mutated sequences shown above the wild type sequences. Both of the p53RE and FXR sites are underlined. Of note, there is 4-bp overlap between these two sites.

Figure 5. siRNAs against p53 reduce EPI-induced UGT2B7 mRNA levels in HepG2 cells. Briefly, 1.5 ml of fresh DMEM containing HepG2 cells ($3x10^5$) was combined with 0.5 ml of serum-free DMEM medium containing 10 µl of Lipofectamine 2000 and 10 ul of either anti-p53 siRNA (20 µM) or nontarget siRNA (20 µM) and subsequently plated into six-well plates. Each transfection was conducted in four wells. 24 h after transfection, the transfection medium was removed and replaced with fresh DMEM medium. 48 h after transfection, cells were harvested from one well of each transfection to prepare whole cell lysate for western blotting assays. The remaining three wells of each transfection were treated with 1 µM EPI or vehicle (0.1% ethanol) for 24 h. Cells were then harvested for total RNA, followed by RT-qPCR to quantify target mRNA. A: shown are representative results from western blotting with an antibody against p53 (top) or β-actin (bottom) in triplicate samples that were transfected with anti-p53 siRNA or non-target siRNA. B: shown is the fold-induction in target gene mRNA levels in EPI-treated and anti-p53 siRNA-transfected HepG2 cells compared to those (set as a value of 1) in vehicle-treated and non-target siRNA-transfected cells, respectively. Data shown are means ± 1 S.D. from a representative experiment of three independent experiments performed in triplicate. ** $p < 0.01$

Molecular Pharmacology Fast Forward. Published on March 28, 2014 as DOI: 10.1124/mol.114.091603
This article has not been copyedited and formatted. The final version may differ from this version.

Figure 6. Nutlin-3α stimulates *UGT2B7* expression and anti-p53 siRNA represses the capacity of nutlin-3α to stimulate *UGT2B7* expression in HepG2 cells. A: HepG2 cells were plated in 6-well plates and cultured for 2-3 days until they reached approximately 80% confluence. Cells were then treated in triplicate with 10 μM Nutlin-3α or vehicle (0.1% ethanol) for 24 h. B: 1.5 ml of fresh DMEM containing HepG2 cells ($3x10^5$) was combined with 0.5 ml of serum-free DMEM medium containing 10 μl of Lipofectamine 2000 and 10 ul of either anti-p53 siRNAs (20 μM) or nontarget siRNAs (20 μM) and subsequently plated into six-well plates. 24 h after transfection, the transfection medium was removed and replaced with fresh DMEM medium. 48 h after transfection, cells were treated with 10 μM Nutlin-3α or vehicle (0.1% ethanol) for 24 h. Total RNA was extracted and reverse-transcribed to generate cDNA, followed by quantitative real-time PCR to quantify target gene mRNA levels. Data are presented as fold-induction in target mRNA levels in nutlin-3α-treated cells (A) and anti-p53 siRNA transfected cells (B) compared to those (set as a value of 1) in vehicle-treated cells (A) and non-target siRNA transfected cells (B), respectively. Data shown are means ± 1 S.D. from a representative experiment of three independent experiments performed in triplicate. * $p < 0.05$, ** $p < 0.01$, ¥ $p > 0.05$

Figure 7. p53 is recruited to the *UGT2B7* proximal promoter upon exposure to EPI or nutlin-3α in HepG2 cells. Cells were treated with 1 μM EPI, 10 μM nutlin-3α, or vehicle (0.1% ethanol) for 24 h and subjected to chromatin immunoprecipitation assays, followed by real-time PCR to quantify the precipitated DNA of target sequences as described under *Materials and Methods*. After normalizing to the data of the negative Control region 2, data were expressed as the -fold enrichment in DNA samples precipitated with the anti-p53 antibody (FL393) compared with that (set as a value of 1) in the control DNA samples

Molecular Pharmacology Fast Forward. Published on March 28, 2014 as DOI: 10.1124/mol.114.091603
This article has not been copyedited and formatted. The final version may differ from this version.

precipitated from equivalent amounts of preimmune IgG serum (IgG). Data shown are means ± 1 S.D. from a representative experiment of three independent experiments performed in triplicates. * $p < 0.05$, ** $p < 0.01$

Figure 8. Known transcription factors and their binding sites which are involved in the regulation of the proximal *UGT2B7* promoter. Shown are five previously reported transcription factors and their binding sites (underlined) and the novel p53RE (boxed) reported in the present study in the *UGT2B7* proximal promoter. Nucleotides of the *UGT2B7* promoter are numbered from the translation initiation ATG codon (bold) with A positioned as "+1". Cdx2, caudual-related homeodomain protein 2; FXR, farnesoid X receptor; HNF, hepatic nuclear factor; p53, tumour suppressor protein p53.

Molecular Pharmacology Fast Forward. Published on March 28, 2014 as DOI: 10.1124/mol.114.091603
This article has not been copyedited and formatted. The final version may differ from this version.

Table 1
Primers used in this study for qPCR, promoter cloning and mutagenesis, and ChIP-qPCR

PCR for cloning	
2B7-1R:	ATACGGTACCTGGTGCAATGCAATGCTTG
2B7-240F:	GCTAGGTACCGCTGAAGGATAGCACTCATA
2B7-283F:	GCATGGGTACCTTGCATAAGACAGATGGCAT
2B7-1046F:	ATAGACGCGTGACCTGAAGGAATACCTCAA
2B7-2076F:	ATGTACGCGTGCCGGTTTCTAAGGCATATA
2B7-3026F:	ATAGACGCGTTCAGCCTCCCACTTTGCAAT
2B7-4026F:	ATCAACGCGTAGTGATGCTTCAGGAAACTT
2B7-4926F:	TACTACGCGTGAGCCCTGTAAACTCTTAAT
Mutagenesis	
2B7-MT1F:	GACACTCTTCTAAAATGCAGTGCATAAGACAGATG
2B7-MT1R:	CATCTGTCTTATGCACTGCATTTTAGAAGAGTGTC
2B7-MT2F:	CTAAAATATATTGCATGGATCAGATGGCATGTCCA
2B7-MT2R:	TGGACATGCCATCTGATCCATGCAATATATTTTAG
2B7-MT3F:	TTGCATAAGACAGATACAGTGTCCATACAAGATC
2B7-MT3R:	GATCTTGTATGGACACTGTATCTGTCTTATGCAA
2B7-MT4F:	ATGTCCATACAAGATGGCAGATATTAGCTGAAGG
2B7-MT4R:	CCTTCAGCTAATATCTGCCATCTTGTATGGACAT
2B7-MT5F:	TACAAGATCCTTGATCGGTGCTGAAGGATAGCAC
2B7-MT5R:	GTGCTATCCTTCAGCACCGATCAAGGATCTTGTA
qPCR	
CYP3A4F:	AGTATGGAAAAGTGTGGGGCT
CYP3A4R:	TGGAGACAGCAATGATCGTAA
p21F:	AGACTCTCAGGGTCGAAAAC
p21R:	TAAGGCAGAAGATGTAGAGC
ChIP-qPCR	
2B7-7906/-7747F:	CCTTCCTTTGGATTTTGGCC
2B7-7906/-7747R:	TGAATGACCTGGGGTGAATT
2B7-355/-209F:	GTTTTGTGTCAAATGGACTGC
2B7-355/-209R:	CCCTTTTATGTTTATGAGTGC
2B7-3026/-2907F:	ATAGACGCGTTCAGCCTCCCACTTTGCAAT
2B7-3026/-2907R:	GCCACTCAGGCACGTGTAGA
CYP3A4F:	TGGCAGAACTTGCCTTCAATT
CYP3A4R:	TGCAGTTGGTGTTGTTCTGCA

Nucleotides of the primers are numbered from the UGT2B7 translation start site ATG codon with the A positioned as "+1". F: Forward; R: reverse; MT, mutation.

Molecular Pharmacology Fast Forward. Published on March 28, 2014 as DOI: 10.1124/mol.114.091603
This article has not been copyedited and formatted. The final version may differ from this version.

Figure 1

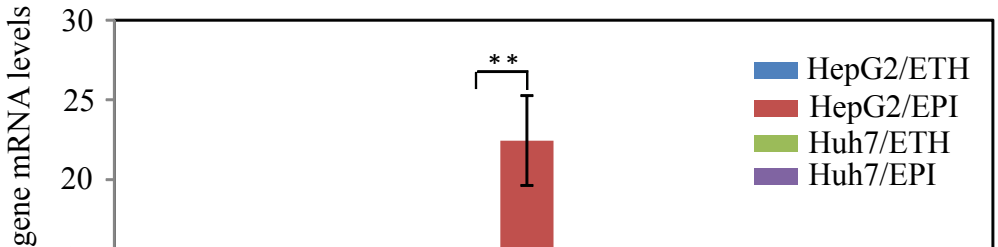

Figure 2

Molecular Pharmacology Fast Forward. Published on March 28, 2014 as DOI: 10.1124/mol.114.091603
This article has not been copyedited and formatted. The final version may differ from this version.

A

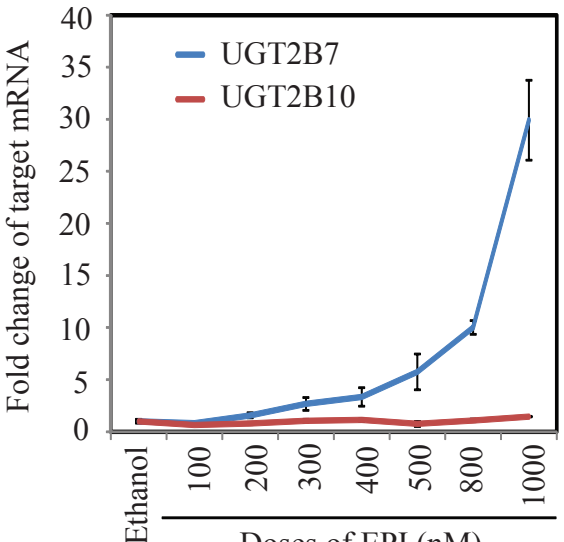

B

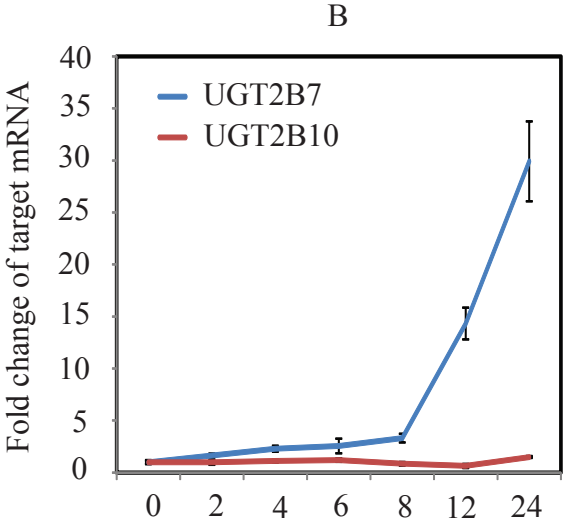

C

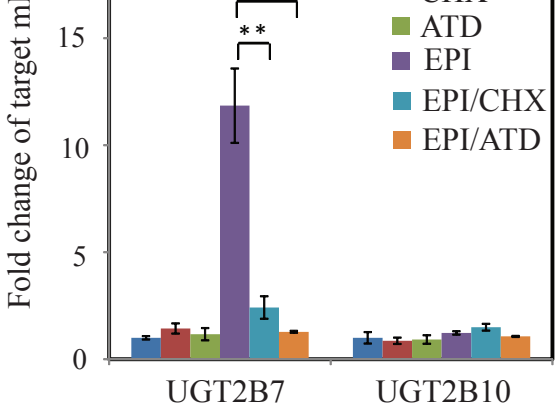

Molecular Pharmacology Fast Forward. Published on March 28, 2014 as DOI: 10.1124/mol.114.091603
This article has not been copyedited and formatted. The final version may differ from this version.

Figure 3

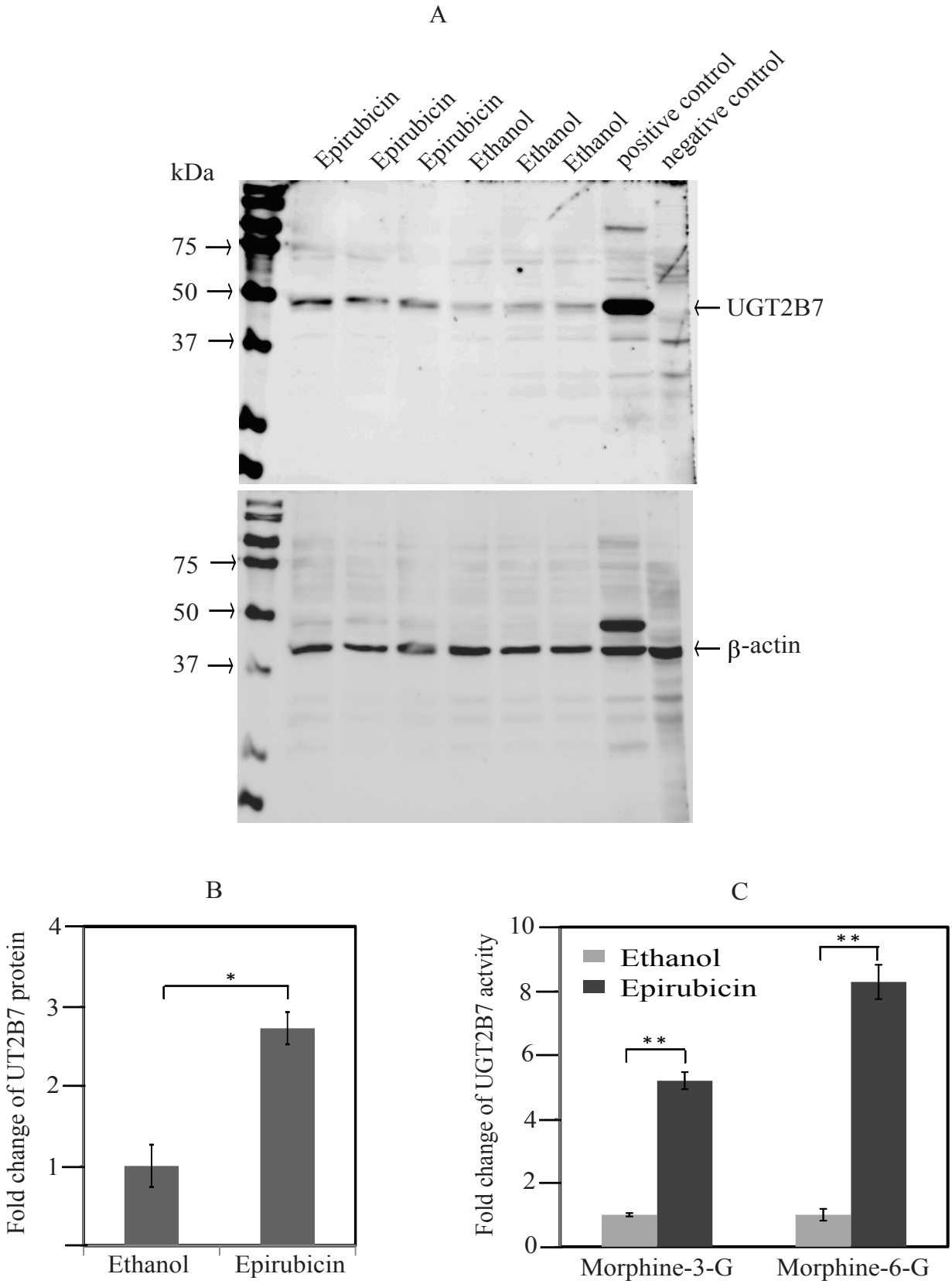

Molecular Pharmacology Fast Forward. Published on March 28, 2014 as DOI: 10.1124/mol.114.091603
This article has not been copyedited and formatted. The final version may differ from this version.

Figure 4

A

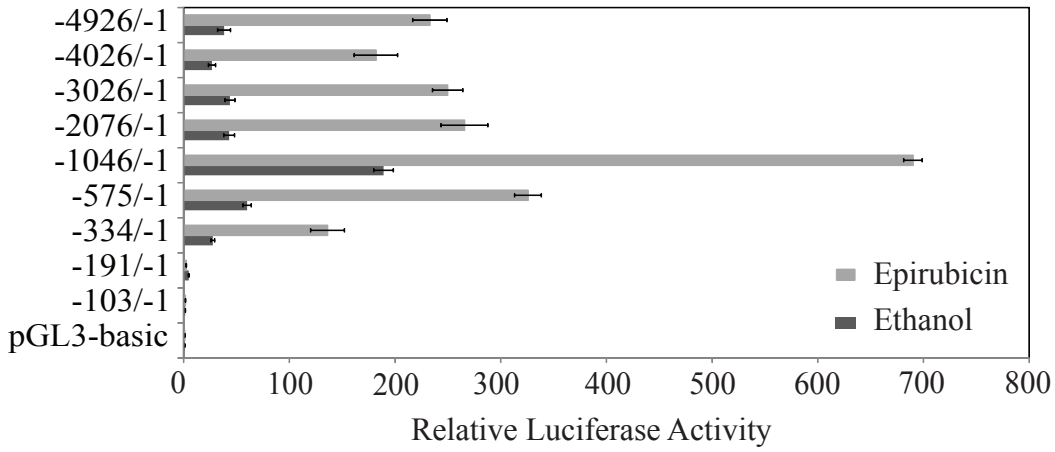

B

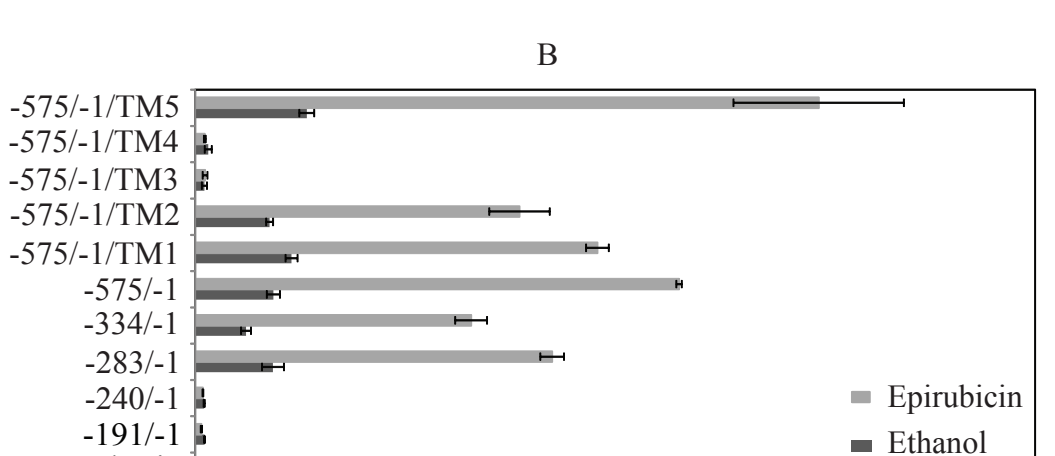

C

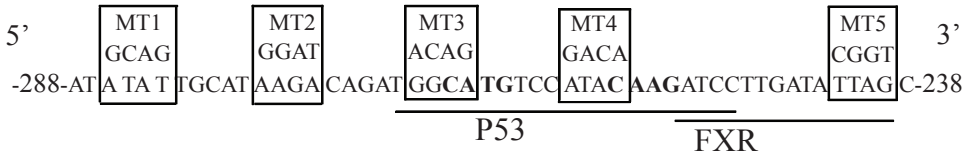

Molecular Pharmacology Fast Forward. Published on March 28, 2014 as DOI: 10.1124/mol.114.091603
This article has not been copyedited and formatted. The final version may differ from this version.

Figure 5

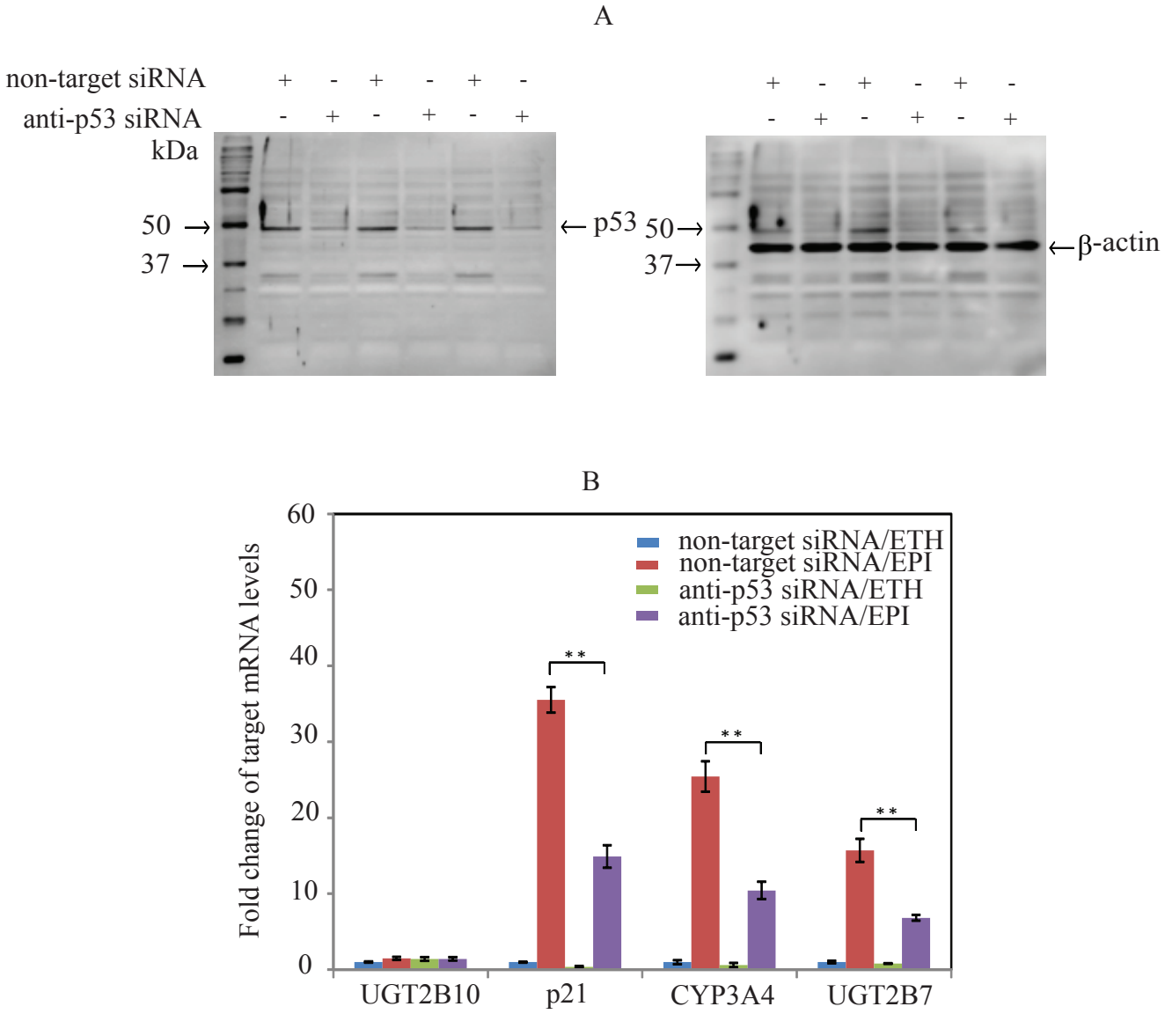

Molecular Pharmacology Fast Forward. Published on March 28, 2014 as DOI: 10.1124/mol.114.091603
This article has not been copyedited and formatted. The final version may differ from this version.

Figure 6

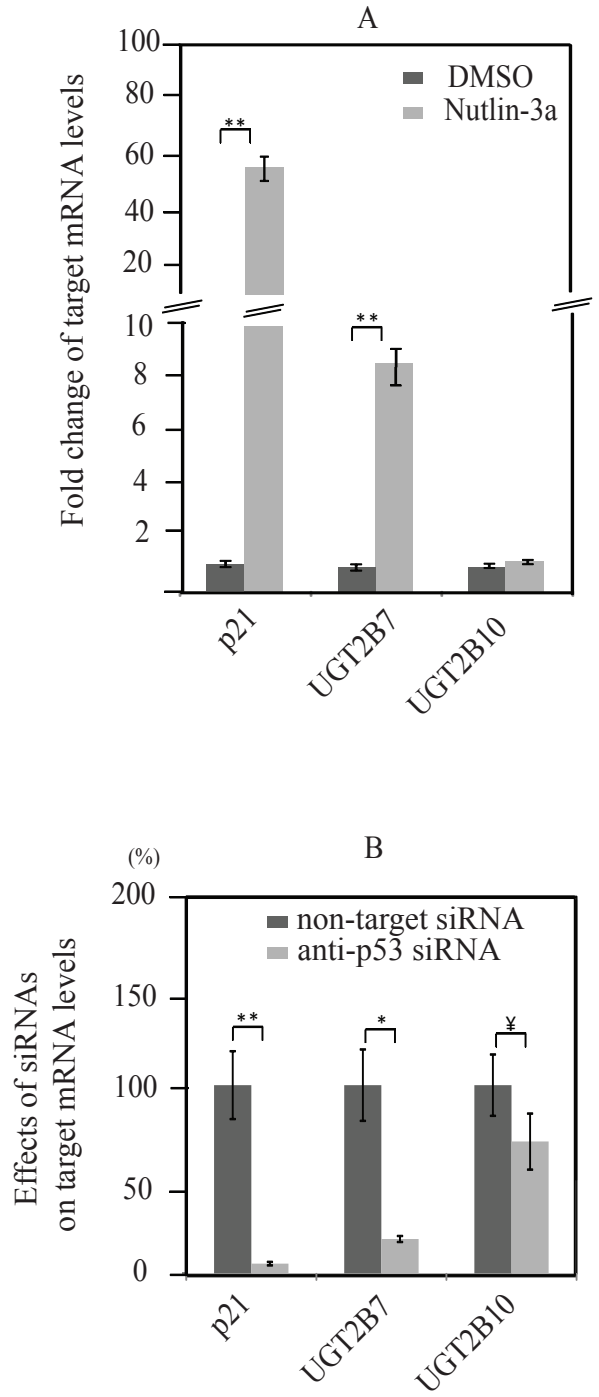

Molecular Pharmacology Fast Forward. Published on March 28, 2014 as DOI: 10.1124/mol.114.091603
This article has not been copyedited and formatted. The final version may differ from this version.

Figure 7

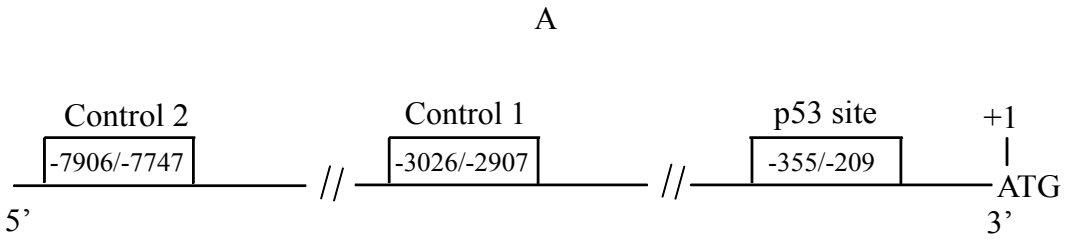

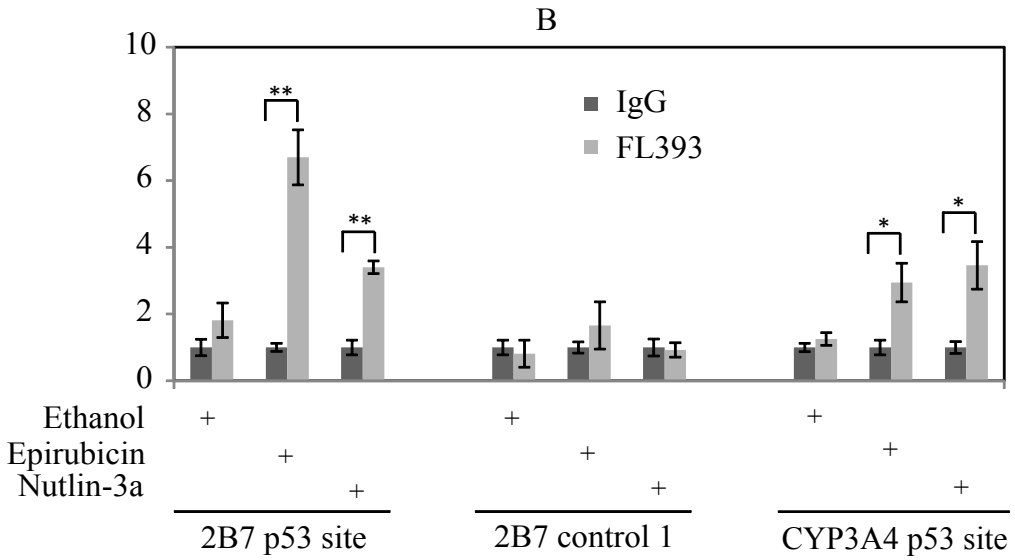

Molecular Pharmacology Fast Forward. Published on March 28, 2014 as DOI: 10.1124/mol.114.091603
This article has not been copyedited and formatted. The final version may differ from this version.

Figure 8